

TP53 Induced Glycolysis and Apoptosis Regulator and Monocarboxylate Transporter 4 drive metabolic reprogramming with c-MYC and NFkB activation in breast cancer

Megan E. Roche¹  | Ying-Hui Ko² | Marina Domingo-Vidal³ | Zhao Lin¹ | Diana Whitaker-Menezes¹ | Ruth C. Birbe⁴ | Madalina Tuluc⁵ | Balázs Győrffy^{6,7} | Jaime Caro⁸ | Nancy J. Philp⁵ | Ramon Bartrons⁹ | Ubaldo Martinez-Outschoorn¹

¹Department of Medical Oncology, Sidney Kimmel Cancer Center, Thomas Jefferson University, Philadelphia, Pennsylvania, USA

²Department of Biochemistry and Molecular Biology, Sidney Kimmel Cancer Center, Thomas Jefferson University, Philadelphia, Pennsylvania, USA

³Immunology, Microenvironment & Metastasis Program, Wistar Institute, Philadelphia, Pennsylvania, USA

⁴Department of Pathology, Cooper University Hospital, Camden, New Jersey, USA

⁵Department of Pathology, Anatomy and Cell Biology, Sidney Kimmel Cancer Center, Thomas Jefferson University, Philadelphia, Pennsylvania, USA

⁶MTA TTK Lendület Cancer Biomarker Research Group, Institute of Enzymology, Budapest, Hungary

⁷Semmelweis University 2nd Department of Pediatrics, Budapest, Hungary

⁸Department of Medicine, Sidney Kimmel Cancer Center, Thomas Jefferson University, Philadelphia, Pennsylvania, USA

⁹Department of Physiological Sciences, University of Barcelona, Barcelona, Spain

Correspondence

Ubaldo Martinez-Outschoorn, Sidney Kimmel Cancer Center Department of Medical Oncology, 233 S. 10th Street, Suite 909, Philadelphia, PA 19107, USA.
 Email: ubaldo.martinez-outschoorn@jefferson.edu

Funding information

National Cancer Institute of the National Institutes of Health (NIH), Grant/Award Numbers: 5P30CA056036-17, K08 CA175193, R37 CA234239; National Institute

Abstract

Breast cancer is composed of metabolically coupled cellular compartments with upregulation of TP53 Induced Glycolysis and Apoptosis Regulator (TIGAR) in carcinoma cells and loss of caveolin 1 (CAV1) with upregulation of monocarboxylate transporter 4 (MCT4) in fibroblasts. The mechanisms that drive metabolic coupling are poorly characterized. The effects of TIGAR on fibroblast CAV1 and MCT4 expression and breast cancer aggressiveness was studied using coculture and conditioned media systems and in-vivo. Also, the role of cytokines in promoting tumor metabolic coupling

Abbreviations: ATP, adenosine triphosphate; BCL2, B-cell lymphoma 2; CAFs, cancer associated fibroblasts; CAV1, caveolin 1; DAB, diaminobenzidine tetrahydrochloride; ETC, electron transport chain; EV, empty vector; Fru-2,6-P₂, fructose-2,6-bisphosphate; HIF-1 α , hypoxia inducible factor 1 alpha; HKII, hexokinase II; HRP, horseradish peroxidase; IHC, immunohistochemistry; IL6, interleukin 6; KD, knockdown; Kla, lacytlysin; KO, knockout; LPS, lipopolysaccharide; MCT1, monocarboxylate transporter 1; MCT4, monocarboxylate transporter 4; MEF, mouse embryonic fibroblast; NADH, nicotinamide adenine dinucleotide (NAD) + hydrogen (H); NADPH, nicotinamide adenine dinucleotide phosphate; NFkB, nuclear factor kappa beta; OCR, oxygen consumption rate; OXPHOS, oxidative phosphorylation; PFK1, phosphofructokinase-1; PFKFB, 6-phosphofructo-2-kinase/fructose-2,6-bisphosphatase; PFKFB3, 6-Phosphofructo-2-Kinase/Fructose-2,6-Biphosphatase 3; PI, propidium iodide; p-Rb, phosphorylated retinoblastoma; ROS, reactive oxygen species; TCA Cycle, tricarboxylic acid cycle; TCGA, The Cancer Genome Atlas; TGFB, transforming growth factor beta; TIGAR, TP53 Induced Glycolysis and Apoptosis Regulator; TMA, tumor microarray; TME, tumor microenvironment; TUNEL, terminal deoxynucleotidyl transferase dUTP nick end labeling; WT, wild-type.

This is an open access article under the terms of the [Creative Commons Attribution-NonCommercial-NoDerivs](#) License, which permits use and distribution in any medium, provided the original work is properly cited, the use is non-commercial and no modifications or adaptations are made.

© 2023 The Authors. *International Journal of Cancer* published by John Wiley & Sons Ltd on behalf of UICC.

of Arthritis and Musculoskeletal and Skin Diseases of the National Institutes of Health (NIH), Grant/Award Number: T32 AR052273; FIS-Fondo de Investigaciones Sanitarias Instituto de Salud Carlos III, Grant/Award Number: PI17/00412; FEDER-Fondo Europeo de Desarrollo Regional (FEDER)

via MCT4 on cancer aggressiveness was studied. TIGAR downregulation in breast carcinoma cells reduces tumor growth. TIGAR overexpression in carcinoma cells drives MCT4 expression and NF_kB activation in fibroblasts. IL6 and TGFB drive TIGAR upregulation in carcinoma cells, reduce CAV1 and increase MCT4 expression in fibroblasts. Tumor growth is abrogated in the presence of MCT4 knockout fibroblasts and environment. We discovered coregulation of c-MYC and TIGAR in carcinoma cells driven by lactate. Metabolic coupling primes the tumor microenvironment allowing for production, uptake and utilization of lactate. In sum, aggressive breast cancer is dependent on metabolic coupling.

KEY WORDS

c-MYC, glycolysis, metabolic heterogeneity, mitochondrial metabolism, monocarboxylate transporter 4, TP53 induced glycolysis and apoptosis regulator

What's new?

Breast cancer is composed of metabolically coupled cellular compartments with upregulation of TIGAR in carcinoma cells and loss of CAV1 and upregulation of MCT4 in fibroblasts. The mechanisms that drive this metabolic coupling remain poorly characterized, however. Here, the authors show that TIGAR expression in carcinoma cells is required to promote tumor growth, which is dependent on the reprogramming of fibroblasts toward upregulation of MCT4 expression and lactate release. Co-regulation of TIGAR, c-MYC and lactate occurs in a carcinoma-cell autonomous fashion, while co-regulation of TIGAR, NF_kB, TGFB and MCT4 unfolds in a paracrine fashion.

1 | INTRODUCTION

Metabolic heterogeneity, or the “Reverse Warburg Effect”, defined as high glycolysis in stromal cells and high OXPHOS in cancer cells, involves an interplay between oncogenes, tumor suppressors, growth factors and cytokines, ultimately promoting cancer aggressiveness.¹⁻¹² High-energy metabolites, such as lactate, can be transferred from glycolytic fibroblasts to carcinoma cells fueling OXPHOS.¹³ To date, the mechanisms driving metabolic heterogeneity have not been well characterized.

TP53 Induced Glycolysis and Apoptosis Regulator (TIGAR) induces metabolic heterogeneity in breast cancer models with increased mitochondrial OXPHOS in carcinoma cells and increased glycolysis in fibroblasts.⁸ TIGAR is a P53 target gene,¹⁴ but its expression is not exclusively dependent on wild-type p53.¹⁴ TIGAR functions as a bisphosphatase and shares similarity with the 6-phosphofructo-2-kinase/fructose-2,6-bisphosphatase (PFKFB) enzymes in the bisphosphatase domain.¹⁵ TIGAR and PFKFB regulate glycolysis via modulation of Fru-2,6-P₂, reducing the affinity of PFK1 for Fru-6-P maintaining ATP-mediated inhibition, regulating PFK1 activity.¹⁵ PFK1 activity, hexokinase activity, glucose import and lactate export are the four rate-limiting steps in glycolytic flux.¹⁶ Reducing PFK1 activity decreases glycolysis.^{14,17} TIGAR expression was inversely related to 2-deoxyglucose uptake using 18-Fluoro 2-deoxy-glucose positron emission tomography.¹⁸ These results validate that TIGAR reduces glycolytic flux. Also, TIGAR binds to and regulates the activity of mitochondrial bound hexokinase II (HKII).^{16,19} In sum, TIGAR targets three rate-limiting

steps in glycolysis, which include glucose uptake, PFK1 and HK activity,^{8,14,16,19} but the underlying mechanisms remain uncharacterized.

TIGAR is highly expressed in many cancer types, driving proliferation, migration, invasion, crosstalk with NF_kB and tumor burden.²⁰⁻²⁵ TIGAR drives breast cancer tumor growth with glycolysis in fibroblasts and utilization of lactate to fuel OXPHOS and ATP production in carcinoma cells.⁸ Together these studies demonstrate TIGAR expression drives cancer progression and aggressiveness, but the mechanisms remain poorly characterized.

In this study, we set out to determine the mechanisms of cross-talk by which TIGAR expression in carcinoma cells induces metabolic heterogeneity and whether carcinoma TIGAR and reciprocal changes in fibroblasts are necessary for aggressive breast cancer. We determined that TIGAR expression in carcinoma cells is required to promote tumor growth, which is dependent upon reprogramming fibroblasts to upregulate MCT4 and lactate release. We discovered a novel coregulation of c-MYC and TIGAR in carcinoma cells.

2 | MATERIALS AND METHODS

2.1 | TIGAR expression in human samples

First, a GEO (<https://www.ncbi.nlm.nih.gov/geo/>) search was performed to identify datasets with published transcriptome-level gene expression data in healthy tissues, using the keywords “gene expression”, “normal” and “GPL96” and “GPL570.” A gene

expression database was set up in a similar method as described.²⁶ For each sample, the raw CEL files were normalized using MAS5. A second scaling normalization was performed using the probe sets present on the GPL96 platform to set the mean expression across all arrays to 1000. For TIGAR, the probe set 219 099 was used. According to JetSet, the 11 probes included in the probe set 219 099_at have a specificity of 0.73 and cover 100% of TIGAR transcripts.²⁷ Differential expression was determined by a Mann-Whitney U test using WinStat for Excel (R.Fitch Software, Bad Krozingen, Germany).

2.2 | TCGA data analysis

Multivariate data analysis of the TCGA breast cancer data segregated on the basis of the highest and lowest quartile of TIGAR expression were analyzed with R (<http://www.R-project.org>) to disclose intrinsic clustering of samples. A Volcano plot was created to assess differentially expressed genes.

2.3 | Cell culture

The human breast carcinoma cell lines T47D (RRID: CVCL_0553), MCF7 (RRID: CVCL_0031) and MDA-MB-231 (RRID: CVCL_0062) were obtained from ATCC (Manassas, VA). The mouse mammary carcinoma cell line AT-3 (RRID: CVCL_VR89), was a generous gift from Dr. Scott Abrams at Roswell Park Cancer Institute. The PY8119 mouse mammary carcinoma (RRID: CVCL_AQ09) cell line was obtained from ATCC. Human skin fibroblasts immortalized with human telomerase reverse transcriptase catalytic domain (hTERT-BJ1) were purchased from Clontech (RRID: CVCL_6573; Mountain View, CA). NIH3T3 cells (RRID: CVCL_0594) were purchased from ATCC. Fibroblasts were generated with green fluorescent protein (BJ1-GFP) overexpression. MEFs were isolated from wild-type and MCT4 knockout (MCT4^{-/-}) mice as described.²⁸ Cell line authentication was performed in December 2022 by ATCC (Manassas, VA). All cell lines were authenticated using short tandem repeat (STR) profiling within the last 3 year. All experiments were performed with mycoplasma-free cells. Cells were treated with 0 to 100 mM lactate for 48 h. Cells were cocultured in a 1:3 carcinoma-to-fibroblast ratio as described.⁸

2.4 | Oxygen consumption rate assessment of tumor microtissue samples

XFe24 Extracellular Flux Analyzer was used with islet capture microplates. Tumors were excised and immediately placed in DMEM growth media on ice. The tumors were cut into uniform 1 mm slices to generate tumor microtissues, which were placed into the center of the islet capture microplate with 100 µl of DMEM growth media. The islet capture screens were inserted with 200 µl of additional growth

media. The microtissues were incubated in non-buffered seahorse media containing 5 mM glucose +/- 10 mM lactate in a CO₂ free incubator for 1 h. The tumor microtissues were subjected to the mito stress test as described.⁸

2.5 | Animal studies

Carcinoma and fibroblast cells were co-injected into female athymic NCr nude mice (NU/NU; Charles River) or C57BL/6 (B6NTac; Taconic) mice as described.⁸ MCT4 wild-type and MCT4^{-/-} mice in the same C57BL/6 (B6NTac; Taconic) background had syngeneic carcinoma and fibroblast cells co-injected as described.²⁹ The Institutional Animal Care and Use Committee (IACUC) approved all animal protocols and all experiments were performed in accordance with National Institutes of Health guidelines and ARRIVE guidelines. Statistical significance was determined by both student *t*-test and the Mann-Whitney U Test.

For non-animal studies Student *T* test was used with *P* value of *P* < .05 being considered statistically significant.

More extensive Materials and Methods can be found in the [Supplementary Material](#).

Graphical Abstract and Study Schematic were created with [BioRender.com](#).

3 | RESULTS

3.1 | Cancer aggressiveness is mediated by TIGAR

To determine the patterns of TIGAR expression in breast cancer, we studied human normal and cancerous tissue datasets. We identified 7623 breast cancer and 76 normal breast samples in GEO. The mean expression of TIGAR was higher in cancer tissues than in normal (mean ± 95% confidence intervals: 514 ± 7 and 390 ± 48 in cancer and normal tissues, respectively, *P* = 3.6E-04), and TIGAR mRNA was 1.4-fold more highly expressed in breast cancer compared with normal breast tissue (Figure 1A). We segregated breast cancer samples from the TGCA on the basis of the highest and lowest quartile of TIGAR expression and calculated T and orthogonal T scores to disclose intrinsic clustering. We found that the samples were strongly segregated based on TIGAR expression (Figure S1A). Next, we assessed the pattern of differentially expressed genes on the basis of TIGAR focusing on the expression of lactate metabolism genes and identified MCT1, LDHB and NDUFA9 as more highly expressed with increased TIGAR expression (Figure S1B-E). We assessed if TIGAR mRNA expression is associated with clinical outcomes. High TIGAR expression in breast cancer is associated with shorter progression free survival (HR = 1.56, *P* = 1.9e-08) and remained significant in the multivariate analyses (Table S1). Since TIGAR is more highly expressed in breast cancer compared with normal breast tissue and is associated with shorter progression free survival, we sought to determine if TIGAR is necessary to induce aggressive breast cancer. In this study we utilized multiple breast cancer and fibroblast models that are expected to have different intrinsic characteristics. We generated

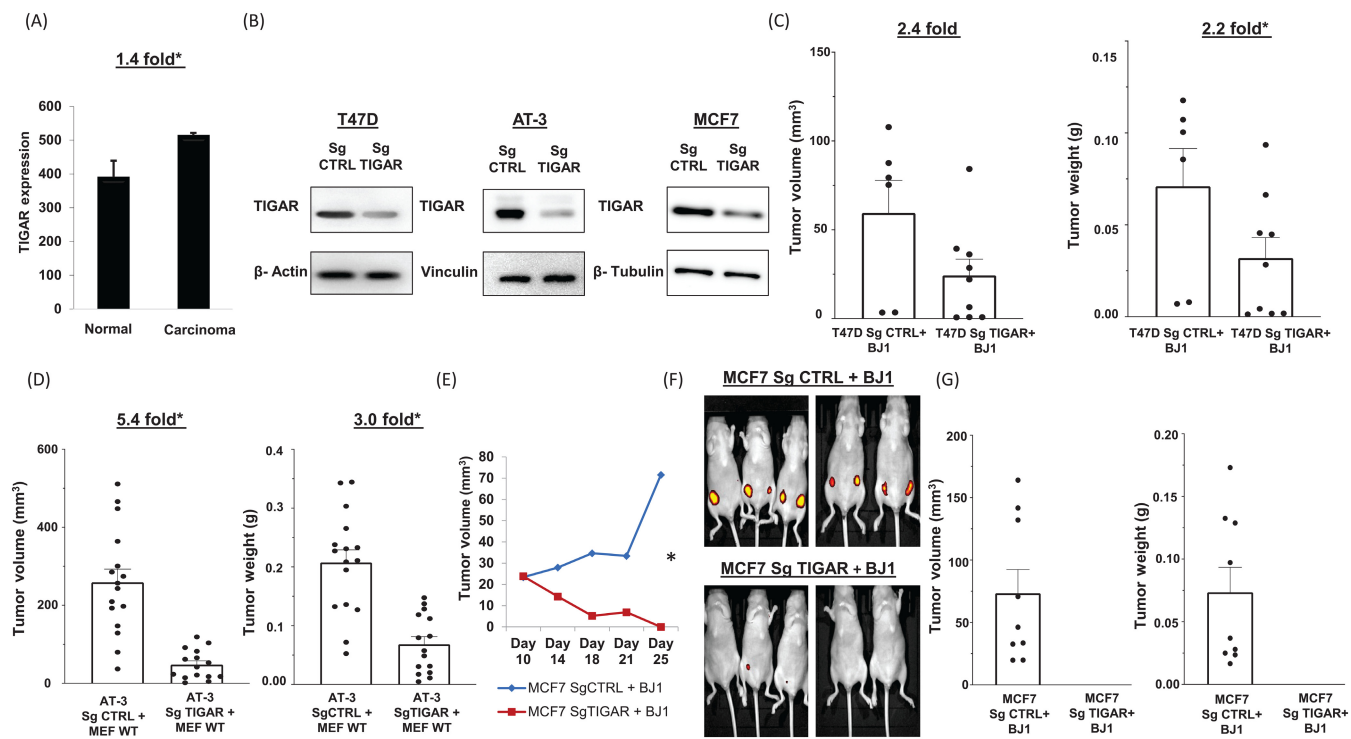


FIGURE 1 TIGAR expression in human breast cancer and effect of TIGAR Knockdown on tumor growth. (A) TIGAR mRNA expression in normal breast tissue and breast cancer. (B) TIGAR immunoblot in T47D, AT-3 and MCF7 carcinoma cells with TIGAR knockdown (sgTIGAR) via CRISPR/Cas9. (C) Tumor volume and weight of TIGAR knockdown T47D cells orthotopically coinjected with BJ1 fibroblasts in nude mice. (D) Tumor volume and weight of TIGAR knockdown AT-3 cells coinjected with MEFs fibroblasts in syngeneic mice. (E-G) Tumor volume and weight of TIGAR knockdown RFP tagged MCF7 cells orthotopically co-injected with BJ1 fibroblasts (E). In vivo imaging for RFP of TIGAR knockdown MCF7 tumors on day 21 after co-injection (F). Tumor volume and weight at resection (G) (*P < .05). Error bars represent the SE of the mean.

TIGAR overexpressing or TIGAR knockdown (KD) cells based on TIGAR, MCT1 and MCT4 expression. Specifically in the murine cell lines we opted for overexpression or downregulation based on TIGAR expression (Figure S2A, B). We generated T47D, AT-3 and MCF7 with TIGAR KD and evaluated its effects on tumor growth (Figure 1B). These cells with TIGAR KD or control were co-injected with BJ1 (human) or MEF (mouse) fibroblasts into female mice. T47D cells with TIGAR KD had a 2.4- and 2.2-fold reduction in tumor volume ($P < .07$) and tumor weight ($P < .05$; Figure 1C). AT-3 cells with TIGAR KD had a 5.4- and 3.0-fold reduction in tumor volume ($P < .05$) and tumor weight ($P < .05$; Figure 1D). TIGAR KD in MCF7-RFP tagged cells co-injected with BJ1 fibroblasts abolished tumor growth compared with control cells ($P < .05$; Figure 1E-G). Specifically, MCF7 Control and TIGAR KD xenografts initially became palpable 10 days post-injection demonstrating engraftment of both conditions (Figure 1E). The MCF7 control xenografts continued to grow over the course of the experiment, but the MCF7 TIGAR KD xenografts completely regressed shown by the tumor growth curves at day 25 and in vivo imaging for RFP at day 21 (Figures 1E-G). The MCF7 control and TIGAR KD cells grew in culture and viability is not compromised suggesting that TIGAR KD cells are unable to endure the tumor microenvironmental pressures. Tumor volume and weight after resection at day 25 are shown in Figure 1G. These data demonstrate that TIGAR knockdown reduces tumor growth.

3.2 | Tumor microenvironment (TME) Fibroblast protein expression effects of carcinoma TIGAR activity

To determine the effects of TIGAR on the tumor microenvironment, carcinoma cells with TIGAR KD or overexpression and controls were cocultured in a system composed of fibroblasts and breast carcinoma cell lines (MCF7, T47D or MDA-MB-231 cells). We assessed if carcinoma cells with TIGAR KD are able to modulate the expression of fibroblast CAV1 since loss of CAV1 induces a CAF phenotype with high glycolysis in fibroblasts. TIGAR KD was able to restore CAV1 expression in BJ1 fibroblasts with a 3.2-fold increase in expression compared with control cells ($P < .05$; Figure S3A). Next, CAV1 was downregulated via shRNA in fibroblasts which decreased TIGAR expression in BJ1 fibroblasts ($P < .05$; Figure S3B). Conversely, TIGAR overexpression in BJ1 fibroblasts led to CAV1 upregulation (Figure S3C). Since TIGAR KD carcinoma cells increased CAV1 expression in fibroblasts, we evaluated the effect of TIGAR overexpression in carcinoma cells on fibroblast CAV1 expression. T47D and MDA-MB-231 TIGAR overexpressing cells reduced fibroblast CAV1 expression 3.3- and 1.5-fold, respectively ($P < .05$; Figure S3D-F). We next modulated TIGAR in carcinoma cells to assess its effects on fibroblast monocarboxylate transporter 4 (MCT4). TIGAR downregulation in carcinoma cells reduced MCT4 expression in BJ1 fibroblasts 1.6-fold

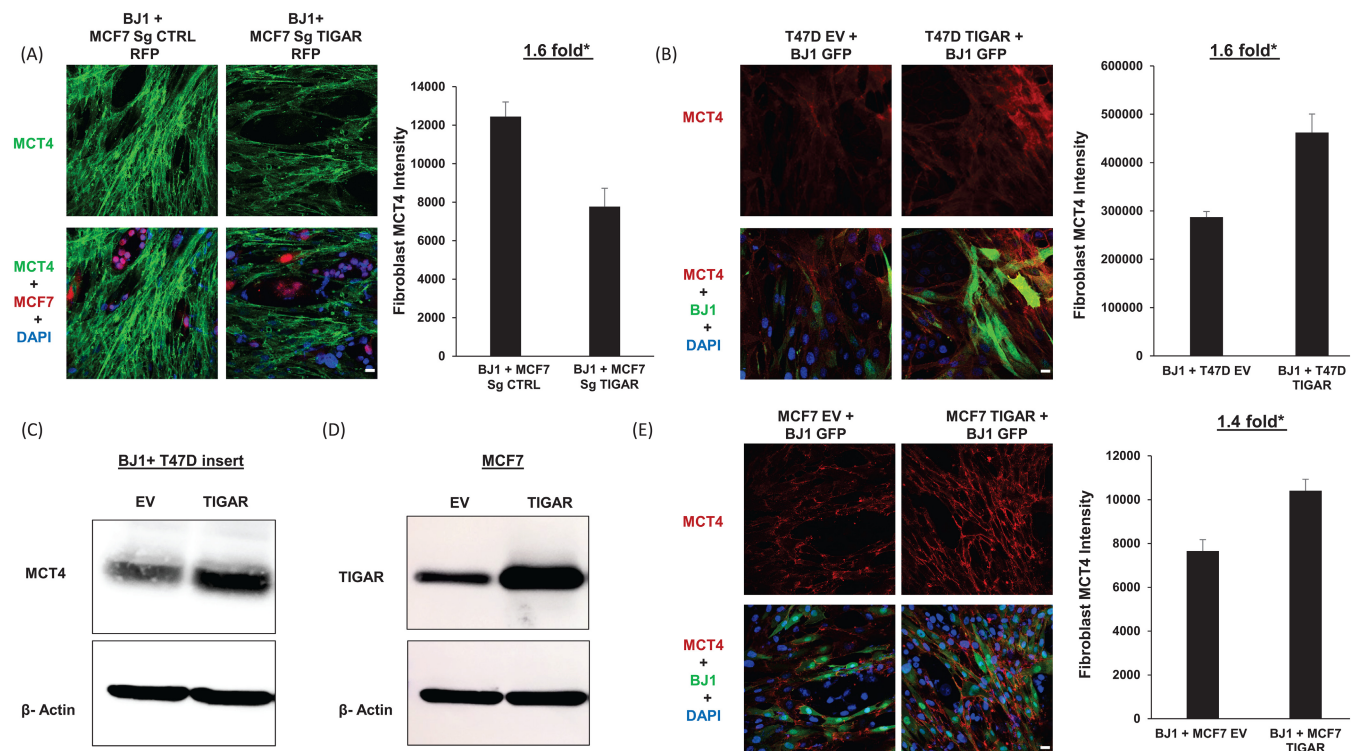


FIGURE 2 Modulation of monocarboxylate transporter 4 (MCT4) in fibroblasts by carcinoma TIGAR. (A, B) MCT4 expression by immunofluorescence in BJ1 fibroblasts cocultured with TIGAR knockdown MCF7 cells (A) and TIGAR overexpression T47D cells (B). (C) MCT4 immunoblot in BJ1 fibroblasts cocultured with TIGAR overexpressing T47D cells via a 0.4 μ m filter insert. Protein from the fibroblast component was immunoblotted for MCT4. (D) TIGAR immunoblot of MCF7 cells overexpressing TIGAR. (E) MCT4 immunofluorescence in BJ1 fibroblasts cocultured with TIGAR overexpressing MCF7 cells. Quantification of fibroblast MCT4 staining is normalized to cell number (* $P < .05$). Error bars represent the SE of the mean. $N = 4$, Scale bar: 20 μ m.

($P < .05$; Figure 2A). Conversely, TIGAR overexpression in T47D and MCF7 carcinoma cells increased MCT4 in BJ1 fibroblasts 1.6- and 1.4-fold, respectively ($P < .05$; Figure 2B-E). Taken together, these data demonstrate that TIGAR expression in carcinoma cells reduces fibroblast CAV1 expression and increases fibroblast MCT4 expression.

We stained a breast cancer-tumor microarray (TMA) for TIGAR and quantified TIGAR staining in carcinoma and stromal cells. Cells staining strongly positive for TIGAR (3+ intensity) by digital pathology quantification were 2.1-fold higher in the carcinoma cells compared with the surrounding stroma ($P < .05$; Figure S4A). To further characterize the compartment specificity of TIGAR expression in carcinoma cells vs fibroblasts, we cocultured PY8119 EV (empty vector control) or PY8119 TIGAR overexpressing breast carcinoma cells with wild-type (WT) MEFs via an insert. We evaluated the expression of TIGAR in the MEFs by immunoblot and found that MEFs cocultured with PY8119 TIGAR overexpressing cells have modestly reduced TIGAR expression compared with MEFs cocultured with PY8119 EV cells (Figure S4B). We next studied the effect of TIGAR on MCT4 expression in fibroblasts in homotypic and coculture with carcinoma cells by immunofluorescence. TIGAR overexpression in fibroblasts reduced MCT4 2.1-fold compared to control cells in homotypic culture ($P < .05$; Figure S4C). In coculture, TIGAR overexpression in

fibroblasts reduced fibroblast MCT4 expression 2-fold ($P < .05$; Figure S4C). To determine the effect of TIGAR overexpression in fibroblasts on tumor growth we co-injected BJ1 fibroblasts overexpressing TIGAR or controls with MDA-MB-231 human breast carcinoma cells. No significant difference in tumor growth was observed between xenografts generated with MDA-MB-231 and fibroblasts overexpressing TIGAR or control ($P > .5$; Figure S4D, E). No significant difference in apoptosis rates was observed in the xenografts generated with MDA-MB-231 and fibroblasts overexpressing TIGAR or control by TUNEL ($P > .2$; Figure S4F). These data demonstrate that the effects of TIGAR expression on tumor growth are compartment-specific, and require carcinoma cell TIGAR expression.

3.3 | TIGAR in carcinoma cells induces NF κ B in fibroblasts

NIH3T3 mouse fibroblasts stably transfected with an NF κ B luciferase reporter were cocultured with control or TIGAR overexpressing carcinoma cells. NF κ B activation is increased 1.4- and 1.2-fold in NIH3T3 fibroblasts cocultured with T47D and MCF7 TIGAR-overexpressing cells ($P < .05$; Figure 3A, B). Coculture activates NF κ B in fibroblasts independently of carcinoma TIGAR expression. Next, we evaluated

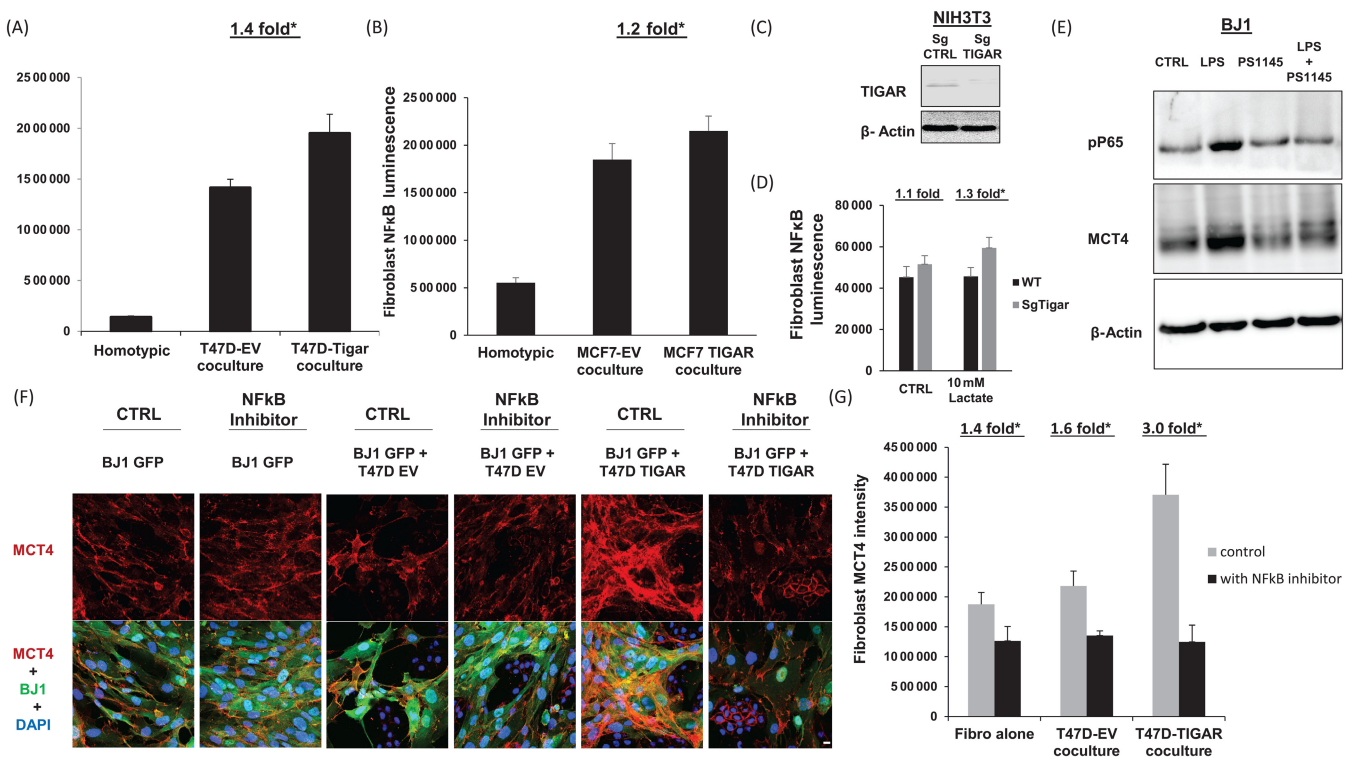


FIGURE 3 NF κ B activation in fibroblasts by carcinoma TIGAR. (A, B) NF κ B activity in NIH3T3 fibroblasts cocultured with TIGAR overexpressing T47D or MCF7 carcinoma cells. NIH3T3 cells were stably transfected with an NF κ B luciferase reporter and luminescence is normalized to total protein. (C) TIGAR immunoblot in NIH3T3 wild-type control or sg TIGAR knockdown fibroblasts. (D) NF κ B activity in NIH3T3 wild-type control or sg TIGAR knockdown fibroblasts under control conditions and after the addition of 10 mM Lactate. NIH3T3 cells were stably transfected with an NF κ B luciferase reporter and luminescence is normalized to total protein. (E) BJ1 fibroblasts were immunoblotted for pP65 and MCT4 after treatment with LPS (1 μ g/ml), NF κ B inhibitor PS1145 (10 μ M) and the combination of LPS and PS1145. (F) MCT4 expression in BJ1 fibroblasts expressing GFP cocultured with TIGAR overexpressing T47D cells with 10 μ M PS1145, which is an NF κ B inhibitor. (G) Quantification of fibroblast MCT4 staining is normalized to cell number (* P < .05). Error bars represent the SE of the mean. N = 4, Scale bar: 20 μ m.

the role of TIGAR expression in fibroblasts on NF κ B activation. NIH3T3 control (WT) or TIGAR KD fibroblasts were stably transfected with the NF κ B luciferase reporter. TIGAR KD in the NIH3T3 cells was verified by immunoblot (Figure 3C). Under control conditions NF κ B activation is not significantly increased in TIGAR KD cells compared with WT cells (P > .05; Figure 3D) but with the addition 10 mM lactate, NF κ B activation is increased 1.3-fold in TIGAR KD cells compared with WT cells (P < .05; Figure 3D). NF κ B drives CAF phenotypes³⁰ and therefore to determine the effect of NF κ B inhibition on fibroblast MCT4 expression, we exposed cells to the NF κ B inhibitor PS1145 (Figure 3E). To validate that PS1145 inhibits NF κ B, BJ1 fibroblasts were exposed to the NF κ B activator lipopolysaccharide (LPS), PS1145 or the combination. NF κ B activity was determined via phospho-p65 immunoblot. LPS increases phospho-p65 expression, but PS1145 blocks phospho-p65 expression (Figure 3E). To determine if MCT4 expression is downstream of NF κ B activation, we evaluated if PS1145 affects MCT4 expression following LPS exposure. LPS treatment was able to upregulate MCT4 expression in fibroblasts, but addition of PS1145 abolished this. Therefore, PS1145 inhibits NF κ B activation and consequently downstream target MCT4 (Figure 3E). NF κ B inhibition via PS1145

reduced MCT4 expression in fibroblasts induced by TIGAR in the carcinoma cells with a 3-fold decrease in fibroblast MCT4 expression (P < .05; Figure 3F, G). Hence, fibroblast NF κ B activation is a mechanism by which carcinoma TIGAR increases fibroblast MCT4 expression.

3.4 | IL6 and TGFB2 induce markers of metabolic coupling in breast cancer, including TIGAR upregulation in carcinoma cells, MCT4 upregulation in fibroblasts and fibroblast CAV1 downregulation

We assessed the production of cytokines in cocultures of carcinoma cells and fibroblasts to determine cytokines that are upregulated (protein) in coculture conditions (Figure 4A). IL6 and TGFB2 increase 75- and 2.0-fold in T47D-BJ1 cocultures compared with carcinoma homotypic cultures (P < .05; Figure 4B, C). IL6 and TGFB2 increase 1.3- and 16-fold, respectively, in T47D-BJ1 cocultures compared with fibroblast homotypic cultures (P < .05; Figure 4B, C). In sum, IL6 and TGFB2 production are upregulated in coculture and high TIGAR conditions in carcinoma cells.

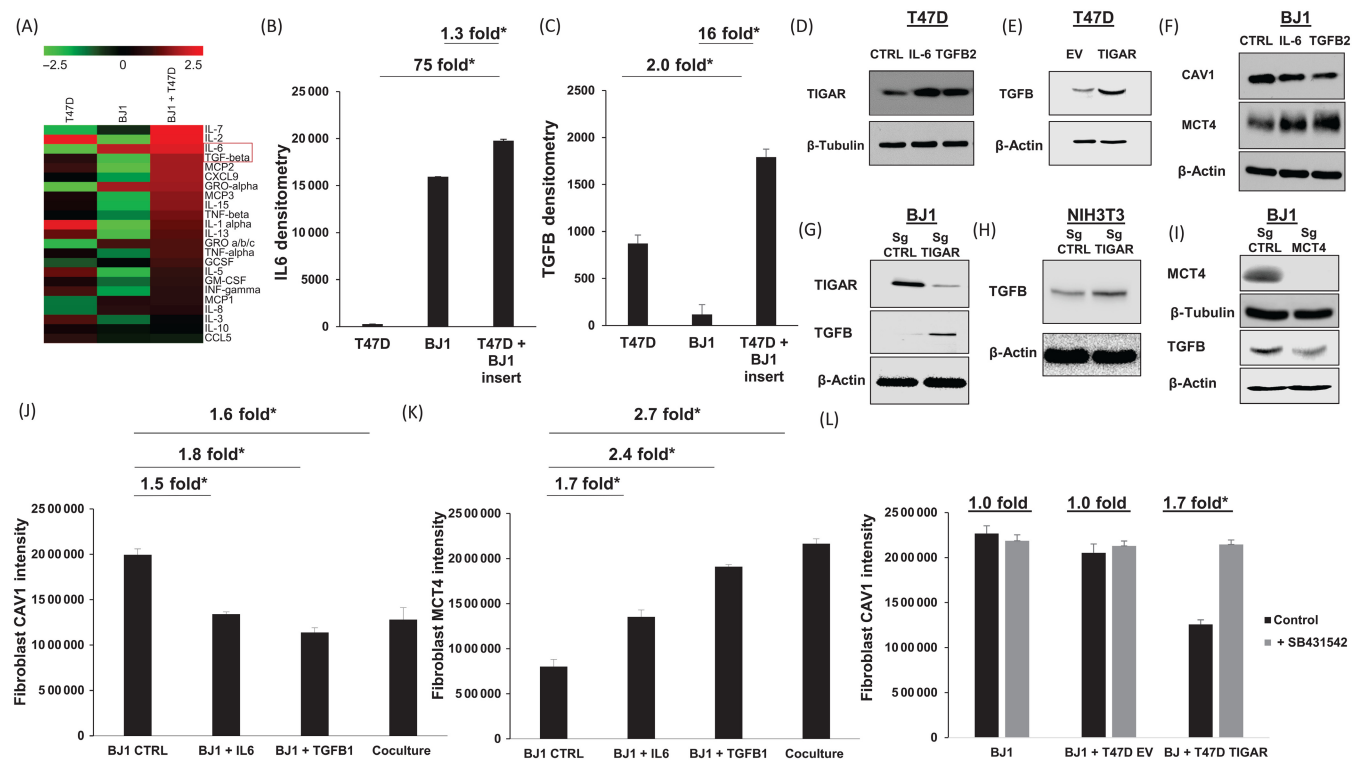


FIGURE 4 Effects of IL6 and TGFB on the expression profile of cancer cells and fibroblasts. (A) Heatmap representation of cytokine expression values determined from conditioned media of T47D carcinoma and BJ1 fibroblast cocultures via an insert. (B) Quantification of IL6 levels in conditioned media from T47D carcinoma and BJ1 fibroblast cocultures via an insert. (C) Quantification of TGFB levels in conditioned media from T47D carcinoma and BJ1 fibroblast cocultures via an insert. (D) TIGAR immunoblot of T47D carcinoma cells exposed to TGFB2 (10 ng/ml) and IL6 (3 ng/ml). (E) TGFB immunoblot in T47D EV empty vector control and TIGAR overexpressing cells. (F) CAV1 and MCT4 immunoblot of BJ1 fibroblast cells exposed to IL6 (3 ng/ml) and TGFB2 (10 ng/ml). (G) TIGAR and TGFB immunoblot in BJ1 Sg CTRL or Sg TIGAR cells. (H) TGFB immunoblot in NIH3T3 Sg CTRL or Sg TIGAR cells. (I) MCT4 and TGFB immunoblot in BJ1 Sg CTRL or Sg MCT4 knockdown cells. (J, K) CAV1 and MCT4 expression by immunofluorescence of BJ1 fibroblasts exposed to the soluble cytokines TGFB2 (10 ng/ml) and IL6 (3 ng/ml) or cocultured with T47D cells. Quantification is normalized to cell number. (L) CAV1 expression by immunofluorescence in BJ1 fibroblasts cocultured with TIGAR overexpressing T47D cells and treated with 10 μM SB431542, which is a TGFB inhibitor. Quantification of fibroblast CAV1 and MCT4 staining is normalized to cell number (*P < .05). Error bars represent the SE of the mean.

We determined the effects of the cytokines IL6 and TGFB on carcinoma TIGAR and fibroblast MCT4 since both of these cytokines are highly expressed in breast cancer, drive aggressiveness, a CAF phenotype, and their expression is upregulated in coculture. TIGAR expression in T47D carcinoma cells was evaluated by immunoblot after treatment with IL6 or TGFB2, and both cytokines increase TIGAR expression (Figure 4D). We also characterized the expression of TGFB in carcinoma cells with TIGAR overexpression by immunoblot, which demonstrated that TGFB expression is upregulated in T47D TIGAR overexpressing cells compared with EV cells (Figure 4E). IL-6 and TGFB2 reduce CAV1 and increase MCT4 expression in BJ1 fibroblasts (Figure 4F). Next, we evaluated the role of IL6 and TGFB2 on fibroblasts, both of which reduce CAV1 and increase MCT4 expression in BJ1 fibroblasts (Figure 4F). TGFB is upregulated in both BJ1 and NIH3T3 TIGAR KD fibroblasts compared with control cells (Figure 4G, H). We evaluated the expression of TGFB in control (Sg CTRL) or MCT4 KD (Sg MCT4) cells. TGFB expression in MCT4 KD cells is downregulated compared with control cells (Figure 4I). CAV1 expression in fibroblasts is reduced by IL6 and TGFB2 1.5-

and 1.8-fold (P < .05; Figure 4J). Also, MCT4 expression is increased in BJ1 fibroblasts with IL6 and TGFB exposure 1.7- and 2.4-fold (P < .05; Figure 4K). Studies have shown that IL6 and TGFB are associated with a CAF phenotype,^{31,32} we exposed cells to the TGFB inhibitor SB431542 to determine the effect of TGFB inhibition on fibroblast CAV1 expression. TGFB inhibition via SB431542 abrogated the CAV1 reduction in fibroblasts induced by TIGAR with a 1.7-fold increase in fibroblast CAV1 expression (P < .05; Figure 4L). Taken together, these data show that TGFB signaling is a mechanism by which TIGAR expression in carcinoma cells modulates CAV1 expression in fibroblasts.

3.5 | MCT4 in fibroblasts drives breast cancer tumor growth

MCT4 knockout (MCT4^{-/-}) mouse embryonic fibroblasts (MEFs) were evaluated for glycolytic flux. MCT4^{-/-} MEFs exhibited 1.6-fold reduced 2-deoxy-glucose uptake as measured by 2-NBDG uptake

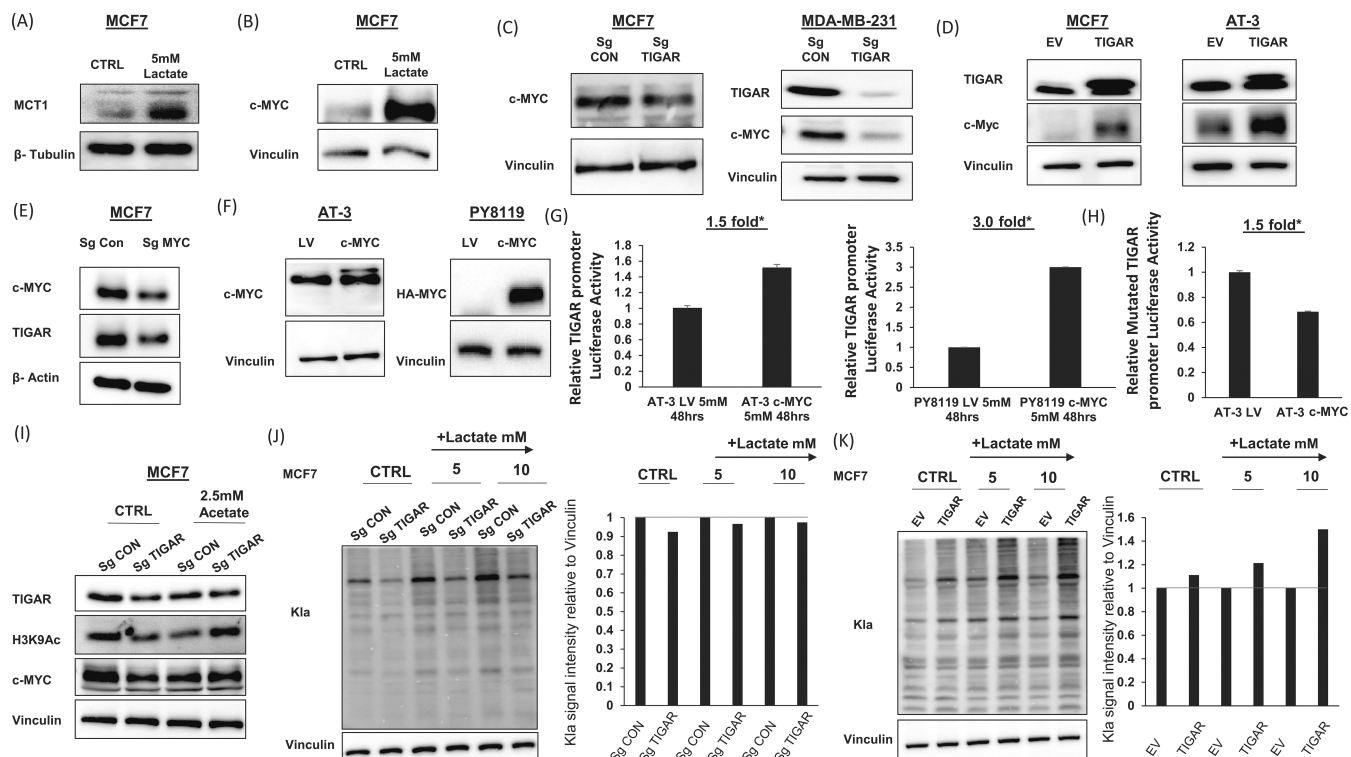


FIGURE 5 Effect of Lactate on carcinoma cell compartment. (A) MCT1 immunoblot in MCF7 cells under control conditions and after treatment with 5 mM lactate. (B) c-MYC immunoblot in MCF7 carcinoma cells exposed to 5 mM Lactate compared with control. (C) c-MYC immunoblot in MCF7 and MDA-MB-231 Sg Control or MCF7 sg TIGAR knockdown cells. (D) c-MYC and TIGAR immunoblot in MCF7 and AT-3 TIGAR overexpressing cells compared with EV empty vector control cells. (E) c-MYC and TIGAR immunoblot in MCF7 Sg MYC knockdown cells compared with Sg Control cells. (F) c-MYC immunoblot in AT-3 and HA-cMYC immunoblot PY8119 in c-MYC overexpressing cells compared with LV control cells. (G) AT-3 and PY8119 LV control and c-MYC overexpressing cells were stably transfected with a secrete-pair dual luminescence GLuc/SEAP TIGAR promoter reporter. The GLuc luminescence is produced based on TIGAR promoter luciferase activity. The GLuc luminescence is normalized to SEAP luminescence which allows for transfection and expression normalization (* $P < .05$). (H) AT-3 LV control and c-MYC overexpressing cells were stably transfected with a secrete-pair dual luminescence GLuc/SEAP mutant TIGAR promoter reporter. The GLuc luminescence is produced based on TIGAR promoter luciferase activity. The GLuc luminescence is normalized to SEAP luminescence which allows for transfection and expression normalization (* $P < .05$). (I) TIGAR, c-MYC and H3K9 acetylation immunoblot in MCF7 Sg Control and Sg TIGAR knockdown cells under control conditions or after exposure to 2.5 mM acetate. (J) Lactyllysine immunoblot in MCF7 Sg control and Sg TIGAR knockdown cells exposed to 0, 5 and 10 mM Lactate. Quantification of Lactyllysine protein expression normalized to vinculin in MCF7 control and TIGAR knockdown cells exposed to lactate. (K) Lactyllysine immunoblot in MCF7 EV empty vector control or TIGAR overexpressing cells exposed to 0, 5 and 10 mM Lactate. Quantification of Lactyllysine protein expression normalized to vinculin in MCF7 control and TIGAR overexpressing cells exposed to lactate. Error bars represent the SE of the mean.

compared with WT ($P < .05$; Figure S5A), which is consistent with reduced glycolytic flux. Lactate release also decreased 6.1-fold in MCT4 $^{−/−}$ MEFs ($P < .05$; Figure S5B). To determine the effect of loss of MCT4 in fibroblasts on tumor growth, we co-injected AT-3 or PY8119 cells with MCT4 $^{−/−}$ or WT MEFs into MCT4 $^{−/−}$ or WT mice. The tumors generated with AT-3 carcinoma cells and MCT4 $^{−/−}$ fibroblasts in MCT4 $^{−/−}$ mice had 1.9-fold smaller volume and 1.6-fold smaller weight ($P < .05$; Figure S5C). The tumors generated with MCT4 $^{−/−}$ MEFs in MCT4 $^{−/−}$ mice have a 1.3-fold increase in apoptotic TUNEL-positive cells compared with the WT ($P < .05$; Figure S5D). A representative image from each condition is shown (Figure S5F). In sum, MCT4 expression in fibroblasts modulates glycolytic flux and absence of MCT4 reduces tumor growth with increased carcinoma cell apoptosis.

tumors generated with MCT4 $^{−/−}$ MEFs in MCT4 $^{−/−}$ mice have a 1.3-fold increase in TUNEL-positive cells compared with the WT ($P < .05$). A representative image from each condition is shown (Figure S5F). In sum, MCT4 expression in fibroblasts modulates glycolytic flux and absence of MCT4 reduces tumor growth with increased carcinoma cell apoptosis.

3.6 | Effect of lactate on cancer cell compartment

Lactate drives TIGAR expression in carcinoma cells.⁸ MCT1 is the main cellular importer of lactate.³¹ We first evaluated if lactate treatment to carcinoma cells, which increases TIGAR expression, also regulates MCT1 expression. Treatment of MCF7 cells with 5 mM lactate

increases MCT1 expression (Figure 5A). Since c-MYC is the main transcription factor that drives MCT1 expression allowing for lactate influx,³³ we wanted to determine the effect of lactate exposure on c-MYC expression in breast carcinoma cells. c-MYC expression was increased in MCF7 after 5 mM lactate treatment (Figure 5B). Since lactate increases both TIGAR and c-MYC expression in breast carcinoma cells, we wanted to evaluate the relationship between c-MYC and TIGAR expression to determine if TIGAR and c-MYC regulate each other. c-MYC expression in TIGAR knockdown cells is reduced compared with control cells (Figure 5C). c-MYC expression was then evaluated by immunoblot in MCF7 and AT-3 EV or TIGAR overexpressing carcinoma cells which demonstrated that increased TIGAR expression increased c-MYC expression (Figure 5D). These data suggest that TIGAR expression can regulate c-MYC expression in breast carcinoma cells. We next wanted to determine if the expression of c-MYC can modulate TIGAR expression. MCF7 cells with Sg control or Sg c-MYC KD cells were evaluated for TIGAR expression and MCF7 c-MYC KD cells have reduced TIGAR expression (Figure 5E). These data suggest that c-MYC and TIGAR regulate each other.

c-MYC by acting as a transcription factor that recognizes a DNA response element (CANNTG) in the promoter of genes directly regulates gene expression. We evaluated the TIGAR promoter sequence and found two E-box elements that c-MYC could bind to and directly regulate TIGAR expression. To determine if c-MYC could be binding to the TIGAR promoter, we generated a luciferase construct containing the TIGAR promoter sequence with both E-Boxes upstream of the luciferase gene. This construct was expressed in LV control or c-MYC overexpressing AT-3 or PY8119 cells (Figure 5F). Cells were treated with 5 mM lactate to enhance c-MYC expression. The TIGAR promoter luciferase activity was increased 1.5- and 3.0-fold in AT-3 and PY8119 c-MYC overexpressing cells ($P < .05$; Figure 5G). We also generated a mutant TIGAR promoter luciferase construct where TIGAR promoter sequence with both E-Boxes mutated is upstream of the luciferase gene. We expressed the mutant TIGAR promoter luciferase construct in LV control or c-MYC overexpressing AT-3 cells. The mutant TIGAR promoter luciferase activity was reduced 1.5-fold in AT-3 c-MYC overexpressing cells ($P < .05$; Figure 5H). These data suggest that c-MYC could be binding directly to the TIGAR promoter driving TIGAR expression. Next, we wanted to evaluate the role of TIGAR driving c-MYC expression via acetylation since c-MYC expression can be regulated by acetylation and epigenetic reprogramming.³⁴ TIGAR overexpressing cells increase mitochondrial metabolism⁸ and presumably TCA cycle flux with increased acetyl-CoA, which can be utilized to acetylate histones with low TIGAR having the opposite effects. Previous studies demonstrated that TIGAR expression is able to drive gene expression via H3K9 acetylation.³⁵ c-MYC expression can be driven by acetylation of H3K9 at its promoter region.³² Therefore, H3K9 acetylation levels in TIGAR KD cells was evaluated by immunoblot analysis under control conditions and after addition of 2.5 mM acetate. Under control conditions, H3K9 acetylation levels are reduced with TIGAR KD, but after addition of acetate, that can be utilized to generate acetyl-CoA, H3K9 acetylation levels are increased (Figure 5I). In TIGAR KD cells, c-MYC expression is reduced, but the

addition of acetate in TIGAR KD cells leads to restoration of c-MYC levels (Figure 5I). Lactylation is a novel epigenetic reprogramming element where the lactyl group from lactate is added to lysine residues of histones and regulates gene expression.³⁶ Since TIGAR and c-MYC expression are regulated by lactate we wanted to evaluate the levels of lactylation in breast carcinoma cells. TIGAR knockdown cells with reduced c-MYC expression were evaluated for lactylation levels by immunoblot and TIGAR knockdown cells have modestly reduced lactylation after 0 to 10 mM lactate treatment compared with controls and lactylation levels increase with lactate (Figure 5J). TIGAR overexpressing cells were evaluated for lactylation levels by immunoblot and TIGAR overexpressing cells have increased lactylation levels after 0 to 10 mM lactate treatment (Figure 5K). We also evaluated the effect of TIGAR overexpression with the addition of 0 to 10 mM lactate on H3K9 acetylation levels. TIGAR overexpressing cells have increased H3K9 acetylation levels, which can be seen at baseline and after addition of lactate (Figure 5A, B). Taken together, these data suggest that there is a direct relationship between TIGAR and c-MYC expression in breast carcinoma cells.

3.7 | TIGAR induced tumor growth is dependent on metabolic reprogramming

We wanted to evaluate the interaction between carcinoma TIGAR and fibroblast MCT4 on tumor growth since TIGAR drives tumor growth, MCT4 expression in fibroblasts drives lactate release, and lactate induces carcinoma TIGAR expression.⁸ PY8119 EV or PY8119 TIGAR overexpressing cells were coinjected with WT or MCT4 $-/-$ MEFs into the flank of WT or MCT4 $-/-$ mice. PY8119 TIGAR overexpressing cells coinjected with WT MEFs in WT mice generated 4.8- and 2.1-fold larger tumors by weight and volume compared with tumors generated with coinjection of PY8119 EV cells ($P < .05$; Figure 6A, B). Coinjection of PY8119 TIGAR overexpressing cells with MCT4 $-/-$ MEFs into MCT4 $-/-$ mice were no longer able to generate larger tumors compared with PY8119 EV coinjection tumors ($P > .05$; Figure 6A, B). Therefore, these data demonstrate that TIGAR's ability to induce larger tumor size is dependent upon fibroblast MCT4.

Tumors were excised and tumor microtissues were generated and subjected to a mitochondrial stress test where oxygen consumption rate (OCR) was measured at baseline, after injection of 1.5 μ M oligomycin, 2.0 μ M FCCP and 0.5 μ M Rotenone/Antimycin A. Oligomycin is a complex V inhibitor that is used to determine ATP-linked OCR and proton leak, FCCP is an ionophore which inhibits ATP synthase and is used to calculate the maximal respiratory capacity, and Rotenone and Antimycin A are complex I and complex III inhibitors that are used to inhibit the electron transport chain to calculate non-mitochondrial OCR.

The OCR of microtissues from PY8119 TIGAR tumors generated with coinjection of WT MEFs in WT mice was measured and the PY8119 TIGAR tumors have no significant change in OCR at baseline, after oligomycin injection, and after FCCP injection in media

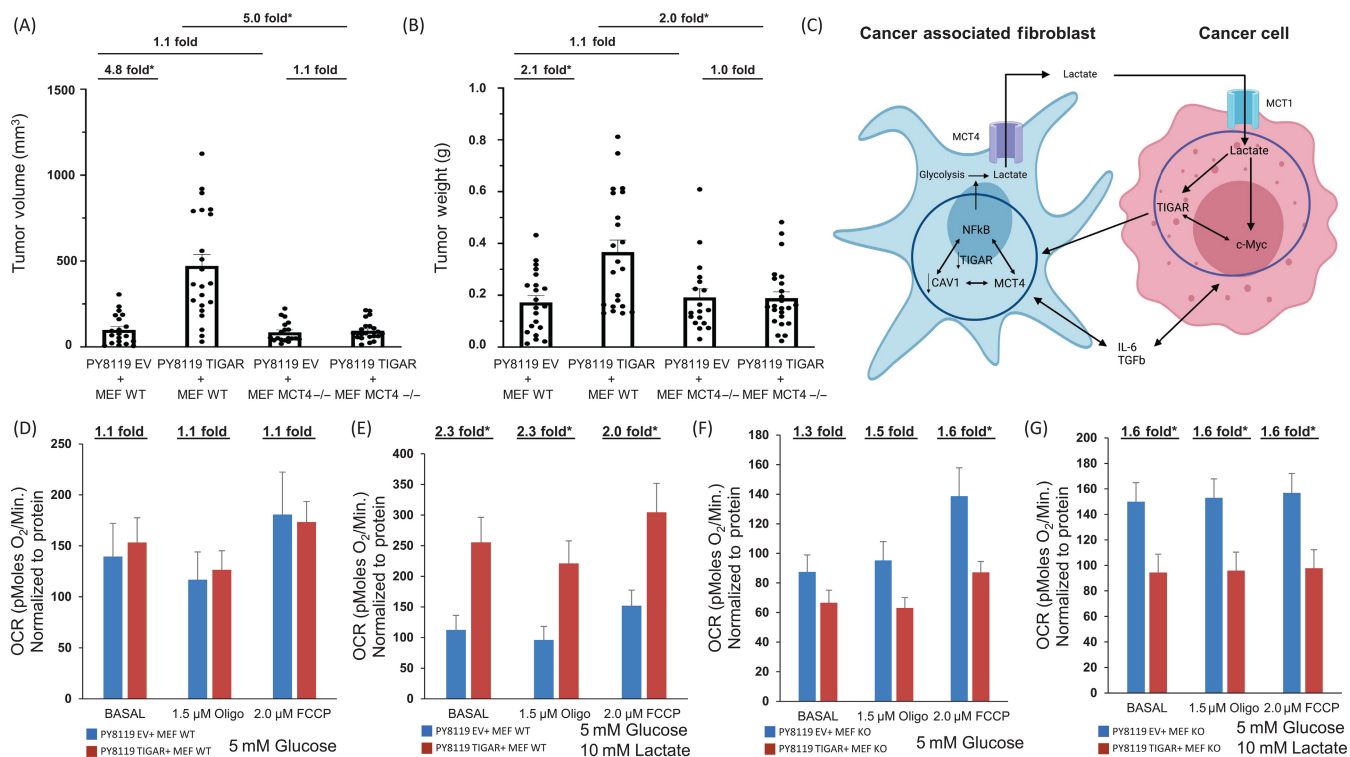


FIGURE 6 Tumor growth and mitochondrial metabolism induced by TIGAR is mediated by MCT4 in fibroblasts. (A, B) Tumor volume and weight of EV empty vector control or TIGAR overexpressing breast carcinoma cells co-injected with wild-type (WT) or MCT4-/- MEFs into the flank of WT or MCT4-/- C57Bl6 mice. (C) Model of effects of TIGAR expression in carcinoma cells. TIGAR in carcinoma cells positively modulates the expression c-MYC in a cell autonomous fashion and modulates the expression of fibroblast MCT4 and CAV1. Conversely, fibroblast MCT4 and CAV1 expression modulates the expression of TIGAR in carcinoma cells. This cross-talk is mediated by the production of the soluble factors TGFB, IL6 and lactate. (D) Oxygen consumption rate (OCR) of tumors generated from PY8119 EV empty vector control or TIGAR overexpressing breast carcinoma cells co-injected with wild-type (WT) MEFs in WT mice was measured under baseline conditions with 5 mM glucose, after injection of 1.5 μM Oligomycin and after injection of 2.0 μM FCCP (N = 6). (E) Oxygen consumption rate (OCR) of tumors generated from PY8119 EV empty vector control or TIGAR overexpressing breast carcinoma cells co-injected with wild-type (WT) MEFs in WT mice was measured under baseline conditions with 5 mM glucose and 10 mM lactate, after injection of 1.5 μM Oligomycin and after injection of 2.0 μM FCCP (N = 6). (F) Oxygen consumption of tumors generated from PY8119 EV empty vector control or TIGAR overexpressing breast carcinoma cells co-injected with MCT4-/- MEFs in MCT4-/- mice was measured under baseline conditions with 5 mM glucose, after injection of 1.5 μM Oligomycin, and after injection of 2.0 μM FCCP (N = 6). G, Oxygen consumption of tumors generated from PY8119 EV empty vector control or TIGAR overexpressing breast carcinoma cells co-injected with MCT4-/- MEFs in MCT4-/- mice was measured under baseline conditions with 5 mM glucose and 10 mM lactate, after injection of 1.5 μM Oligomycin, and after injection of 2.0 μM FCCP (N = 6). OCR values were normalized to protein concentration. Error bars represent the SE of the mean. (*P < .05). Created with BioRender.com

containing only 5 mM glucose compared with PY8119 EV tumors coinjected with WT MEFs in WT mice (P > .05; Figure 6D). PY8119 TIGAR tumors generated with WT MEFs in WT mice have 2.3-fold increased OCR at baseline, 2.3-fold increased OCR after oligomycin injection, 2.0-fold increased OCR after FCCP injection in media containing 5 mM glucose and 10 mM lactate compared with PY8119 EV empty vector control tumors coinjected with wild-type MEFs in WT mice (P < .05; Figure 6E). PY8119 TIGAR tumors generated with MCT4-/- MEFs in MCT4-/- mice have no significant change in OCR at baseline (P > .05), after oligomycin injection (P > .05), and reduce OCR after FCCP injection in media containing only 5 mM glucose (P < .05) compared with PY8119 EV tumors generated with MCT4-/- MEFs in MCT4-/- mice (Figure 6F). To determine if the reduced OCR in PY8119 TIGAR tumors generated with MCT4-/-

MEFs in MCT4-/- mice can be rescued by the addition of lactate to the media, the mitochondrial stress test was performed on the tumor microtissues with media containing 5 mM glucose and 10 mM lactate. PY8119 TIGAR tumors generated with MCT4-/- MEFs in MCT4-/- mice have 1.6-fold reduced OCR at baseline (P < .05), 1.6-fold reduced OCR after oligomycin injection (P < .05), and 1.6-fold reduced OCR after FCCP injection (P < .05) in media containing 5 mM glucose and 10 mM lactate compared with PY8119 EV tumors with coinjection of MCT4-/- MEFs in MCT4-/- mice (Figure 6G). Taken together, these data demonstrate that tumors generated with PY8119 TIGAR and WT MEFs in WT mice have increased OCR in vivo and this is dependent upon lactate and MCT4 in fibroblasts. Tumors generated with PY8119 TIGAR cells and MCT4-/- MEFs in MCT4-/- mice cannot increase OCR upon exposure to lactate suggesting that there

is metabolic reprogramming occurring in the tumors, which cannot be overcome by the addition of lactate. In sum, metabolic heterogeneity and lactate in the TME is required for TIGAR mediated tumor growth and a model is shown in Figure 6C.

We wanted to evaluate if providing exogenous lactate is sufficient to restore the TIGAR mediated tumor growth in the MCT4^{−/−} background. PY8119 TIGAR overexpressing carcinoma cells were coinjected with MCT4^{−/−} MEFs into MCT4^{−/−} mice. Mice were treated with systemic lactate (500 mg/kg) or vehicle control by IP injection daily until tumor excision. PY8119 TIGAR tumors generated with MCT4^{−/−} MEFs in MCT4^{−/−} mice and treated with lactate were not statistically different by tumor volume or weight ($P > .05$; Figure S7A). The blood lactate concentration of the mice was measured after IP injection. The blood lactate concentration in the MCT4^{−/−} mice treated with lactate was 2.1-fold greater than vehicle control MCT4^{−/−} mice ($P < .05$; Figure S7B). To evaluate if exogenous lactate treatment has any effect on TIGAR mediated tumor growth in the WT background, PY8119 TIGAR overexpressing cells were coinjected with WT MEFs into WT mice and treated with systemic lactate (500 mg/kg) or vehicle control by IP injection daily until tumor excision. PY8119 TIGAR tumors generated with WT MEFs in WT mice and treated with lactate generated 3.2- and 1.6-fold larger tumors by weight and volume ($P < .05$; Figure S7C). The blood lactate concentration of the WT mice was measured after IP injection. The blood lactate concentration in the WT mice treated with lactate was 2.0-fold greater than vehicle control treated WT mice ($P < .05$; Figure S7D). Finally, knockdown for MCT4 in BJ1 fibroblasts reduces expression of TIGAR in MCF7 carcinoma cells separated by an insert (Figure S8A). These data suggest that there is metabolic reprogramming occurring in the tumors that allows TIGAR overexpressing tumors to uptake and utilize lactate in WT conditions to promote tumor growth. In MCT4^{−/−} conditions, the metabolism of the tumors is reprogrammed in a way that abolishes TIGAR's ability to uptake and utilize lactate, preventing TIGAR mediated tumor growth. We also determined that exogenous lactate treatment is not sufficient to rescue TIGAR mediated tumor growth in an MCT4^{−/−} background. Taken together, these data demonstrate that lactate in the TME is required for TIGAR mediated tumor growth and that TIGAR induces metabolic priming in the TME, which allows for the production, uptake, and utilization of lactate by carcinoma cells within the tumor.

4 | DISCUSSION

Our results demonstrate that TIGAR expression in carcinoma cells induces metabolic heterogeneity by upregulating MCT4 and downregulating CAV1 in fibroblasts. CAV1 downregulation increases glycolysis and HIF1A stabilization in fibroblasts.^{37,38} MCT4 is a proton-coupled lactate transporter, which mainly exports lactate,³⁹ allowing for glycolytic fibroblasts to release lactate. The current study adds to a body of research demonstrating that TIGAR modulates glycolysis via the rate limiting steps; PFK1 and HKII activity^{14,19} and glucose uptake and lactate release.¹⁸ We describe for the first time that

TIGAR in carcinoma cells increases MCT4 expression in fibroblasts. TIGAR knockdown cells lose the ability to modulate the fibroblast expression of MCT4 and CAV1 to promote tumor growth. The effects of TIGAR on breast cancer aggressiveness are compartment-specific, TIGAR overexpression in carcinoma cells but not fibroblasts drives aggressiveness.⁸

We determined the mechanisms of crosstalk between carcinoma cells overexpressing TIGAR and fibroblasts that induces metabolic heterogeneity. TIGAR expression in carcinoma cells induces an inflammatory environment, promoting fibroblast NFkB activation and production of the cytokines IL6 and TGFB2. This leads to the upregulation of MCT4 and downregulation of CAV1 in fibroblasts, as well as upregulation of TIGAR in carcinoma cells.

The current study demonstrates that the induction of metabolic heterogeneity between carcinoma cells and fibroblasts is a mechanism by which TIGAR induces tumor aggressiveness. MEFs from MCT4^{−/−} mice have reduced glycolysis. Coculture of carcinoma cells with MCT4 KD fibroblasts reduces TIGAR expression (Figure S8A). Coculture of carcinoma cells with MCT4 KD fibroblasts reduces carcinoma TIGAR expression. MCT4^{−/−} MEFs co-injected with carcinoma cells in MCT4^{−/−} mice have reduced tumor growth compared with carcinoma cells co-injected with WT MEFs in WT mice. These data suggest that MCT4 mediated transfer high-energy metabolites, such as lactate, from glycolytic fibroblasts to carcinoma cells fueling OXPHOS is important for tumor growth. Carcinoma cells cocultured with fibroblasts also have increased expression of the lactate importer MCT1, which allows for the uptake of lactate that can fuel OXPHOS.⁴⁰

Lactate induces cancer aggressiveness,³¹ accompanied by TIGAR upregulation.⁸ We studied the role of lactate and TIGAR on c-MYC expression, the main transcription factor that drives MCT1 expression for import into carcinoma cells, mitochondrial metabolism, and biogenesis.^{12,33,41} We observed that lactate upregulates c-MYC expression in carcinoma cells, a feature of aggressive breast cancer.^{42,43}

Here, we discovered a novel coregulation of c-MYC and TIGAR, suggesting that c-MYC may be directly regulating TIGAR expression via binding to the TIGAR promoter. Additionally, TIGAR may be regulating c-MYC by epigenetic reprogramming. Further studies are necessary to evaluate the mechanisms by which TIGAR and c-MYC regulate each other. Furthermore, we found that TIGAR not only reprograms carcinoma cell metabolism, but also reprograms fibroblasts to express MCT4, which is required to drive tumor growth and cancer aggressiveness. Coinjections of PY8119 TIGAR overexpressing cells with WT MEFs in WT mice generated significantly larger tumors than those generated from EV control cells. However, the growth advantage induced by TIGAR is abolished when TIGAR overexpressing cells are injected with MCT4^{−/−} MEFs in MCT4^{−/−} mice. Measurements of oxygen consumption rates (OCR) from tumor microtissues demonstrated that TIGAR overexpressing tumors in WT mice have increased mitochondrial metabolism, which is abolished with coinjection with MCT4^{−/−} MEFs in MCT4^{−/−} mice. Exogenous lactate treatment is not sufficient to rescue tumor growth in the MCT4^{−/−} background.

Overall, we found that metabolic heterogeneity and reprogramming of both carcinoma cells and fibroblasts with high TME lactate are required for TIGAR-mediated tumor growth. We uncovered a new relationship between TIGAR, c-MYC and lactate in carcinoma cells and between TIGAR, NFkB, TGFB and MCT4 in fibroblasts.

AUTHOR CONTRIBUTIONS

Megan E. Roche, Ying-Hui Ko, Jaime Caro, Nancy J. Philp, Ramon Bartrons, and Ubaldo Martinez-Outschoorn were involved in study design and concept. Megan E. Roche, Ying-Hui Ko, Marina Domingo-Vidal, Zhao Lin, Diana Whitaker-Menezes, Balázs Győrffy were involved in data acquisition. Megan E. Roche, Ying-Hui Ko, Marina Domingo-Vidal, Zhao Lin, Diana Whitaker-Menezes, Ruth C. Birbe, Madalina Tuluc, Balázs Győrffy, Jaime Caro, Ramon Bartrons, Ubaldo Martinez-Outschoorn were involved in data analysis and interpretation. Megan E. Roche and Ubaldo Martinez-Outschoorn drafted the manuscript. Megan E. Roche, Diana Whitaker-Menezes, Jaime Caro, Nancy J. Philp, Ramon Bartrons, and Ubaldo Martinez-Outschoorn edited the manuscript. The work reported in the paper has been performed by the authors, unless clearly specified in the text. All authors have read and approved of its submission to this journal.

ACKNOWLEDGMENTS

We would like to thank Dr. Jose Martinez for the thoughtful discussions about this work. We would also like to thank Dr. Mark Fortini for reviewing this manuscript. The following Sidney Kimmel Cancer Center Shared Resources supported by 5P30CA056036-17 were used to conduct this research: Bioimaging Shared Resource, Lab Animal Shared Resource, Translational Pathology Shared Resource, and Flow Cytometry Shared Resource Facility.

FUNDING INFORMATION

National Institute of Arthritis and Musculoskeletal and Skin Diseases of the National Institutes of Health (NIH) under Award Number T32 AR052273 (Megan E. Roche), National Cancer Institute of the National Institutes of Health (NIH), under Award Numbers K08 CA175193 and R37 CA234239 (Ubaldo Martinez-Outschoorn) and 5P30CA056036-17, which supports the FIS-Fondo de Investigaciones Sanitarias Instituto de Salud Carlos III [PI17/00412] and FEDER-Fondo Europeo de Desarrollo Regional (FEDER) (Ramon Bartrons) supported this work.

CONFLICT OF INTEREST STATEMENT

The authors declare that they have no conflict of interest.

DATA AVAILABILITY STATEMENT

All data generated or analyzed during this study are included in this article. The data sets used and/or analyzed during the current study are available from the corresponding author on reasonable request. Data sources and handling of the publicly available datasets used in this study are described in the Materials and Methods (Supplementary Material) and in Table S1. Further details and other data that support the findings of this study are available from the corresponding authors upon request.

ETHICS STATEMENT

The Institutional Animal Care and Use Committee (IACUC) at Thomas Jefferson University approved all animal protocols (01875, 01607). All experiments were performed in accordance with National Institutes of Health guidelines and the study is reported in accordance with ARRIVE guidelines. Only female mice were used in this study.

ORCID

Megan E. Roche <https://orcid.org/0000-0002-8887-2895>

REFERENCES

- Koukourakis MI, Giatromanolaki A, Harris AL, Sivridis E. Comparison of metabolic pathways between cancer cells and stromal cells in colorectal carcinomas: a metabolic survival role for tumor-associated stroma. *Cancer Res.* 2006;66(2):632-637. doi:[10.1158/0008-5472.CAN-05-3260](https://doi.org/10.1158/0008-5472.CAN-05-3260)
- Soneveaux P, Végran F, Schroeder T, et al. Targeting lactate-fueled respiration selectively kills hypoxic tumor cells in mice. *J Clin Invest.* 2008;118(12):3930-3942. doi:[10.1172/JCI36843](https://doi.org/10.1172/JCI36843)
- Pavlides S, Whitaker-Menezes D, Castello-Cros R, et al. The reverse Warburg effect: aerobic glycolysis in cancer associated fibroblasts and the tumor stroma. *Cell Cycle.* 2009;8(23):3984-4001. doi:[10.4161/cc.8.23.10238](https://doi.org/10.4161/cc.8.23.10238)
- Nieman KM, Kenny HA, Penicka CV, et al. Adipocytes promote ovarian cancer metastasis and provide energy for rapid tumor growth. *Nat Med.* 2011;17(11):1498-1503.
- Fiaschi T, Marini A, Giannoni E, et al. Reciprocal metabolic reprogramming through lactate shuttle coordinately influences tumor-stroma interplay. *Cancer Res.* 2012;72(19):5130-5140. doi:[10.1158/0008-5472.CAN-12-1949](https://doi.org/10.1158/0008-5472.CAN-12-1949)
- Brauer HA, Makowski L, Hoadley KA, et al. Impact of tumor microenvironment and epithelial phenotypes on metabolism in breast cancer. *Clin Cancer Res.* 2013;19(3):571-585. doi:[10.1158/1078-0432.CCR-12-2123](https://doi.org/10.1158/1078-0432.CCR-12-2123)
- Goodwin ML, Jin H, Straessler K, et al. Modeling alveolar soft part sarcomagenesis in the mouse: a role for lactate in the tumor microenvironment. *Cancer Cell.* 2014;26(6):851-862. doi:[10.1016/j.ccr.2014.10.003](https://doi.org/10.1016/j.ccr.2014.10.003)
- Ko YH, Domingo-Vidal M, Roche M, et al. TP53-inducible glycolysis and apoptosis regulator (TIGAR) metabolically reprograms carcinoma and stromal cells in breast cancer. *J Biol Chem.* 2016;291(51):26291-26303. doi:[10.1074/jbc.M116.740209](https://doi.org/10.1074/jbc.M116.740209)
- Sousa CM, Biancur DE, Wang X, et al. Pancreatic stellate cells support tumour metabolism through autophagic alanine secretion. *Nature.* 2016;536(7617):479-483. doi:[10.1038/nature19084](https://doi.org/10.1038/nature19084)
- Diehl K, Dinges LA, Helm O, et al. Nuclear factor E2-related factor-2 has a differential impact on MCT1 and MCT4 lactate carrier expression in colonic epithelial cells: a condition favoring metabolic symbiosis between colorectal cancer and stromal cells. *Oncogene.* 2018;37(1):39-51. doi:[10.1038/onc.2017.299](https://doi.org/10.1038/onc.2017.299)
- Lyssiotis CA, Kimmelman AC. Metabolic interactions in the tumor microenvironment. *Trends Cell Biol.* 2017;27(11):863-875. doi:[10.1016/j.tcb.2017.06.003](https://doi.org/10.1016/j.tcb.2017.06.003)
- Martinez-Outschoorn UE, Peiris-Pages M, Pestell RG, Sotgia F, Lisanti MP. Cancer metabolism: a therapeutic perspective. *Nat Rev Clin Oncol.* 2017;14(1):11-31. doi:[10.1038/nrclinonc.2016.60](https://doi.org/10.1038/nrclinonc.2016.60)
- Penkert J, Ripperger T, Schieck M, Schlegelberger B, Steinemann D, Illig T. On metabolic reprogramming and tumor biology: a comprehensive survey of metabolism in breast cancer. *Oncotarget.* 2016;7(41):6762-67649. doi:[10.18632/oncotarget.11759](https://doi.org/10.18632/oncotarget.11759)
- Bensaad K, Tsuruta A, Selak MA, et al. TIGAR, a p53-inducible regulator of glycolysis and apoptosis. *Cell.* 2006;126(1):107-120. doi:[10.1016/j.cell.2006.05.036](https://doi.org/10.1016/j.cell.2006.05.036)

15. Bartrons R, Simon-Molas H, Rodriguez-Garcia A, et al. Fructose 2,6-bisphosphate in cancer cell metabolism. *Front Oncol.* 2018;8:331. doi:[10.3389/fonc.2018.00331](https://doi.org/10.3389/fonc.2018.00331)
16. Tanner LB, Goglia AG, Wei MH, et al. Four key steps control glycolytic flux in mammalian cells. *Cell Syst.* 2018;7(1):49-62 e48. doi:[10.1016/j.cels.2018.06.003](https://doi.org/10.1016/j.cels.2018.06.003)
17. Bensaad K, Cheung EC, Vousden KH. Modulation of intracellular ROS levels by TIGAR controls autophagy. *EMBO J.* 2009;28(19):3015-3026. doi:[10.1038/emboj.2009.242](https://doi.org/10.1038/emboj.2009.242)
18. Zhou X, Xie W, Li Q, et al. TIGAR is correlated with maximal standardized uptake value on FDG-PET and survival in non-small cell lung cancer. *PLoS One.* 2013;8(12):e080576. doi:[10.1371/journal.pone.0080576](https://doi.org/10.1371/journal.pone.0080576)
19. Cheung EC, Ludwig RL, Vousden KH. Mitochondrial localization of TIGAR under hypoxia stimulates HK2 and lowers ROS and cell death. *Proc Natl Acad Sci USA.* 2012;109(50):20491-20496. doi:[10.1073/pnas.1206530109](https://doi.org/10.1073/pnas.1206530109)
20. Wei M, Peng J, Wu P, et al. Prognostic value of TIGAR and LC3B protein expression in nasopharyngeal carcinoma. *Cancer Manag Res.* 2018;10:5605-5616. doi:[10.2147/CMAR.S175501](https://doi.org/10.2147/CMAR.S175501)
21. Zhao M, Fan J, Liu Y, et al. Oncogenic role of the TP53-induced glycolysis and apoptosis regulator in nasopharyngeal carcinoma through NF-kappaB pathway modulation. *Int J Oncol.* 2016;48(2):756-764. doi:[10.3892/ijo.2015.3297](https://doi.org/10.3892/ijo.2015.3297)
22. Tang Y, Kwon H, Neel BA, et al. The fructose-2,6-bisphosphatase TIGAR suppresses NF-kappaB signaling by directly inhibiting the linear ubiquitin assembly complex LUBAC. *J Biol Chem.* 2018;293(20):7578-7591. doi:[10.1074/jbc.RA118.002727](https://doi.org/10.1074/jbc.RA118.002727)
23. Cheung EC, Athineos D, Lee P, et al. TIGAR is required for efficient intestinal regeneration and tumorigenesis. *Dev Cell.* 2013;25(5):463-477. doi:[10.1016/j.devcel.2013.05.001](https://doi.org/10.1016/j.devcel.2013.05.001)
24. Peña-Rico MA, Calvo-Vidal MN, Villalonga-Planells R, et al. TP53 induced glycolysis and apoptosis regulator (TIGAR) knockdown results in radiosensitization of glioma cells. *Radiother Oncol.* 2011;101(1):132-139. doi:[10.1016/j.radonc.2011.07.002](https://doi.org/10.1016/j.radonc.2011.07.002)
25. Maurer GD, Heller S, Wanka C, Rieger J, Steinbach JP. Knockdown of the TP53-induced glycolysis and apoptosis regulator (TIGAR) sensitizes glioma cells to hypoxia, irradiation and Temozolomide. *Int J Mol Sci.* 2019;20(5):1-14. doi:[10.3390/ijms20051061](https://doi.org/10.3390/ijms20051061)
26. Gyorffy B, Schafer R. Meta-analysis of gene expression profiles related to relapse-free survival in 1,079 breast cancer patients. *Breast Cancer Res Treat.* 2009;118(3):433-441. doi:[10.1007/s10549-008-0242-8](https://doi.org/10.1007/s10549-008-0242-8)
27. Li Q, Birkbak NJ, Gyorffy B, Szallasi Z, Eklund AC. Jetset: selecting the optimal microarray probe set to represent a gene. *BMC Bioinformatics.* 2011;12:474. doi:[10.1186/1471-2105-12-474](https://doi.org/10.1186/1471-2105-12-474)
28. Domingo-Vidal M, Whitaker-Menezes D, Martos-Rus C, et al. Cigarette smoke induces metabolic reprogramming of the tumor stroma in head and neck squamous cell carcinoma. *Mol Cancer Res.* 2019;17(9):1893-1909. doi:[10.1158/1541-7786.MCR-18-1191](https://doi.org/10.1158/1541-7786.MCR-18-1191)
29. Bissetto S, Whitaker-Menezes D, Wilski NA, et al. Monocarboxylate transporter 4 (MCT4) knockout mice have attenuated 4NQO induced carcinogenesis; a role for MCT4 in driving oral squamous cell cancer. *Front Oncol.* 2018;8:324. doi:[10.3389/fonc.2018.00324](https://doi.org/10.3389/fonc.2018.00324)
30. Erez N, Truitt M, Olson P, Hanahan D. Cancer-associated fibroblasts are activated in incipient neoplasia to orchestrate tumor-promoting inflammation in an NF-κB-dependent manner. *Cancer Cell.* 2010;17(2):135-147. doi:[10.1016/j.ccr.2009.12.041](https://doi.org/10.1016/j.ccr.2009.12.041)
31. Fisher DT, Appenheimer MM, Evans SS. The two faces of IL-6 in the tumor microenvironment. *Semin Immunol.* 2014;26(1):38-47. doi:[10.1016/j.smim.2014.01.008](https://doi.org/10.1016/j.smim.2014.01.008)
32. Calon A, Tauriello DV, Battle E. TGF-beta in CAF-mediated tumor growth and metastasis. *Semin Cancer Biol.* 2014;25:15-22. doi:[10.1016/j.semcan.2013.12.008](https://doi.org/10.1016/j.semcan.2013.12.008)
33. Doherty JR, Yang C, Scott KE, et al. Blocking lactate export by inhibiting the Myc target MCT1 disables glycolysis and glutathione synthesis. *Cancer Res.* 2014;74(3):908-920. doi:[10.1158/0008-5472.CAN-13-2034](https://doi.org/10.1158/0008-5472.CAN-13-2034)
34. Wu H, Yang TY, Li Y, et al. Tumor necrosis factor receptor-associated factor 6 promotes hepatocarcinogenesis by interacting with histone deacetylase 3 to enhance c-Myc gene expression and protein stability. *Hepatology.* 2020;71:148-163.
35. Zhou W, Zhao T, Du J, Ji G, Li X, et al. TIGAR promotes neural stem cell differentiation through acetyl-CoA-mediated histone acetylation. *Cell Death Dis.* 2019;10:198.
36. Zhang D, Tang Z, Huang H, et al. Metabolic regulation of gene expression by histone lactylation. *Nature.* 2019;574:575-580.
37. Martinez-Outschoorn UE, Sotgia F, Lisanti MP. Caveolae and signalling in cancer. *Nat Rev Cancer.* 2015;15(4):225-237. doi:[10.1038/nrc3915](https://doi.org/10.1038/nrc3915)
38. Asterholm IW, Mundy DI, Weng J, Anderson RG, Scherer PE. Altered mitochondrial function and metabolic inflexibility associated with loss of caveolin-1. *Cell Metab.* 2012;15(2):171-185. doi:[10.1016/j.cmet.2012.01.004](https://doi.org/10.1016/j.cmet.2012.01.004)
39. Brooks GA. The science and translation of lactate shuttle theory. *Cell Metab.* 2018;27(4):757-785. doi:[10.1016/j.cmet.2018.03.008](https://doi.org/10.1016/j.cmet.2018.03.008)
40. Wallace DC. Mitochondria and cancer. *Nat Rev Cancer.* 2012;12(10):685-698. doi:[10.1038/nrc3365](https://doi.org/10.1038/nrc3365)
41. Agarwal E, Altman BJ, Seo JH, et al. Myc-mediated transcriptional regulation of the mitochondrial chaperone TRAP1 controls primary and metastatic tumor growth. *J Biol Chem.* 2019;294:10407-10414. doi:[10.1074/jbc.AC119.008656](https://doi.org/10.1074/jbc.AC119.008656)
42. Green AR, Aleskandarany MA, Agarwal D, et al. MYC functions are specific in biological subtypes of breast cancer and confers resistance to endocrine therapy in luminal tumours. *Br J Cancer.* 2016;114(8):917-928. doi:[10.1038/bjc.2016.46](https://doi.org/10.1038/bjc.2016.46)
43. Smith JC, Sheltzer JM. Systematic identification of mutations and copy number alterations associated with cancer patient prognosis. *eLife.* 2018;7:1-26. doi:[10.7554/eLife.39217](https://doi.org/10.7554/eLife.39217)

SUPPORTING INFORMATION

Additional supporting information can be found online in the Supporting Information section at the end of this article.

How to cite this article: Roche ME, Ko Y-H, Domingo-Vidal M, et al. TP53 Induced Glycolysis and Apoptosis Regulator and Monocarboxylate Transporter 4 drive metabolic reprogramming with c-MYC and NFkB activation in breast cancer. *Int J Cancer.* 2023;153(9):1671-1683. doi:[10.1002/ijc.34660](https://doi.org/10.1002/ijc.34660)